
CosPGD: a unified white-box adversarial attack for pixel-wise prediction tasks

Shashank Agnihotri
Visual Computing Group
University of Siegen
Germany

Steffen Jung
Max Planck Institute for Informatics
Saarland Informatics Campus
Germany

Margret Keuper
University of Siegen, and
Max Planck Institute for Informatics
Saarland Informatics Campus
Germany

Abstract

While neural networks allow highly accurate predictions in many tasks, their lack of robustness towards even slight input perturbations hampers their deployment in many real-world applications. Recent research towards evaluating the robustness of neural networks such as the seminal *projected gradient descent* (PGD) attack and subsequent works have drawn significant attention, as they provide an effective insight into the quality of representations learned by the network. However, these methods predominantly focus on image classification tasks, while only a few approaches specifically address the analysis of pixel-wise prediction tasks such as semantic segmentation, optical flow, disparity estimation, and others, respectively. Thus, there is a lack of a unified adversarial robustness benchmarking tool (algorithm) that is applicable to all such pixel-wise prediction tasks. In this work, we close this gap and propose CosPGD, a novel white-box adversarial attack that allows optimizing dedicated attacks for any pixel-wise prediction task in a unified setting. It leverages the cosine similarity between the distributions over the predictions and ground truth (or target) to extend directly from classification tasks to regression settings. We outperform the *SotA* on semantic segmentation attacks in our experiments on PASCAL VOC2012 and CityScapes. Further, we set a new benchmark for adversarial attacks on optical flow, and image restoration displaying the ability to extend to any pixel-wise prediction task.

1 Introduction

Neural networks (NNs) have been gaining popularity for estimating solutions to various complex tasks including numerous vision tasks like classification [34, 26, 60, 38], semantic segmentation [46, 64], or disparity [37] and optical flow [17, 29, 52] estimation. However, NNs are inherently black-box function approximators [5], known to find shortcuts to map the input to a target distribution [20] or to learn biases [19]. Thus we have limited information on the quality of representations learned by the network and despite their highly accurate predictions in many tasks, neural network based models tend to lack robustness towards even slight input perturbations. This draws skepticism on the real-world applicability of neural networks.

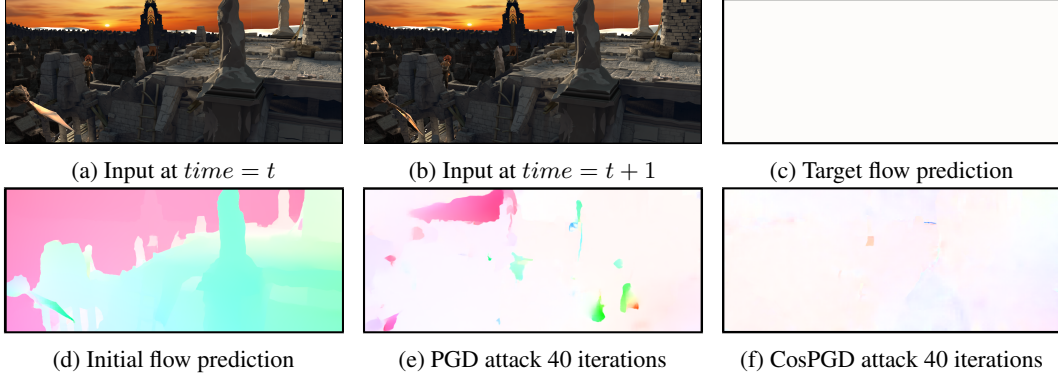


Figure 1: A comparison of optical flow predictions using RAFT [52] on Sintel [6, 59] validation images changed due to targeted PGD attack in Fig. 1e to targeted CosPGD attack in Fig. 1f w.r.t. the initial flow prediction shown in Fig. 1d. Fig. 1c shows the optical flow target viz. a zero vector. Figs. 1a and 1b show 2 consecutive frames for which the optical flow was predicted. For the same perturbation size and amount of iterations, the proposed CosPGD alters the estimated optical flow more strongly and brings it to almost a $\vec{0}$.

Recent research towards evaluating the robustness of neural networks such as FGSM [21], the *projected gradient descent* (PGD) attack [36] and subsequent works such as [50, 11, 12] and benchmarks [14] have therefore attracted significant attention.

An adversarial attack adds a crafted, small (epsilon-sized) perturbation to the input of a neural network that aims to alter the prediction. Due to the practical relevance to evaluate and analyze neural network models, such attacks have been extensively developed and studied [21, 36, 58, 39, 42, 35]. Yet, existing approaches predominantly focus on attacking image classification models. However, arguably, the robustness of models for pixel-wise prediction tasks is highly relevant for many safety-critical applications such as motion estimation in autonomous driving or medical image segmentation. The application of existing attacks to pixel-wise prediction tasks such as semantic segmentation or optical flow estimation is possible in principle (e.g. as in [3]), albeit carrying only limited information since the pixel-specific loss information is not leveraged. In Figure 1, we illustrate this effect on the task of a targeted attack on optical flow estimation and show that global attacks such as PGD (see Figure 1(e)) can fool the network predictions to some extent. However, it tends to only fit the target in a limited amount of locations. Recently, Gu et al. [22] showed that harnessing pixel-wise information for adversarial attacks leads to much stronger attacks for semantic segmentation tasks. They argue that, during the attack, the loss to be backpropagated needs to be rescaled such that already flipped pixel predictions are less important. Thus, SegPGD [22] makes a binary decision for each pixel based on the predicted class at this location to compute the gradient to be leveraged for the attack. While this works well for semantic segmentation tasks, it can not extend to pixel-wise regression tasks by definition.

In this work, we propose CosPGD, a novel white-box adversarial attack. CosPGD uses the cosine-similarity between the prediction and target for each pixel, to generate an adversarial attack. Due to its principled formulation, CosPGD can be used for a wide range of pixel-wise prediction tasks, beyond semantic segmentation. Figure 1(f) shows its effect on optical flow estimation, where it can fit the target at almost all locations. CosPGD uses the pixel-precise loss information is therefore significantly stronger than global attacks like PGD. Since it can leverage the posterior distribution of the prediction for the loss computation, it can significantly outperform SegPGD on semantic segmentation. The main contributions of this work are as follows:

- We propose a novel white-box adversarial attack, CosPGD as a benchmarking tool that can be used to attack all pixel-wise prediction tasks, including semantic segmentation as well as optical flow prediction, and thus allow to evaluate their robustness in a unified setting.
- For semantic segmentation, we compare our method to another recently proposed adversarial attack, SegPGD that also uses pixel-wise information for generating attacks but is limited to pixel-wise classification task. CosPGD can outperform SegPGD by a significant margin.

- The proposed CosPGD can be used as a *targeted* attack and as a *non-targeted* attack. We provide implementations for both l_2 and l_∞ bounded CosPGD attacks to allow for a wide range of evaluation scenarios.
- To demonstrate that CosPGD is widely applicable and can in-principle extend to all pixel-wise prediction tasks (classification and regression), we also evaluate CosPGD as a l_∞ bounded targeted attack on optical flow estimations and image restoration tasks.

2 Related work

The vulnerability of NNs to adversarial attacks was first explored in [21] for image classification, proposing the Fast Gradient Sign Method (FGSM). FGSM is a single-step (one-iteration) white-box adversarial attack that perturbs the input in the direction of its gradient, generated from backpropagating the loss, with a small step size, such that the model prediction becomes incorrect. Due to its fast computation, it is still a widely used approach. Numerous subsequent works have been directed towards generating effective adversarial attacks for diverse tasks including NLP [43, 45, 31], or 3D tasks [62, 51]. Yet, the high input dimensionality of image classification models results in the striking effectiveness of adversarial attacks in this field [21]. A vast line of work has been dedicated to assessing the quality and robustness of representations learned by the network, including the curation of dedicated evaluation data for particular tasks [32, 27, 28] or the crafting of effective adversarial attacks. Patch attacks perturb a localized region in the image (e.g. [4]), while methods such as proposed in [21, 36, 39, 58, 42, 11, 2, 7, 47] argue in a Lipschitz continuity motivated way that a robust network’s prediction should not change drastically if the perturbed image is within the epsilon-ball of the original image and thus optimize attacks globally within the epsilon neighborhood of the original input. Our proposed CosPGD approach follows this line of work.

White-box attacks assume full access to the model and its gradients [21, 36, 39, 58, 22, 42] while black-box attacks optimize the perturbation in a randomized way [2, 30]. The proposed CosPGD derives its optimization objective from Projected Gradient Descent PGD [36] and is a white-box attack.

Further, one distinguishes between *targeted attacks* (e.g. [57, 18, 49]) that turn the network predictions towards a specific target and *untargeted attacks* that optimize the attack to cause any incorrect prediction. PGD [36], and CosPGD by extension, allows for both settings [54].

While previous attacks predominantly focus on classification tasks, only a few approaches specifically address the analysis of pixel-wise prediction tasks such as semantic segmentation, optical flow, or disparity estimation. For example, PCFA [49] was applied to the estimation of optical flow and specifically minimizes the average end-point error (*AEE*) to a target flow field. A notable exception of pixel-wise white-box adversarial attack is proposed in [22]. The recent SegPGD [22] attack could showcase the importance of pixel-wise attacks for semantic segmentation. In this work, we propose CosPGD to provide a principled benchmarking tool for adversarial attacks, that can be applied to a wide range of pixel-wise prediction tasks.

Similar to SegPGD, the here proposed CosPGD is based on the optimization formulated in Projected Gradient Descent (PGD) [36]. PGD in its formulation is very similar to FGSM, i.e. it aims to increase the network’s loss for an image by adding epsilon-bounded noise. Yet, it is significantly more expensive to optimize than FGSM since it is allowed not one but multiple optimization steps. We explain PGD in more detail in Section 3. SegPGD [22] extends upon PGD for semantic segmentation by considering the loss per pixel. For effective optimization, it splits the model’s predicted segmentation mask into correctly classified and incorrectly classified pixels, by comparing it to the ground truth segmentation mask. Thus, the loss is scaled over the iterations and the attack does not continue to increase the loss on already flipped pixel labels. While SegPGD improves upon previous adversarial attacks, it is limited to pixel-wise *classification* tasks (i.e. semantic segmentation) by definition and cannot be extended to regression-based tasks like disparity estimation or optical flow estimation. Thus, we propose CosPGD. CosPGD uses the pixel-wise cosine similarity between the distribution over the predictions and the distribution over the targets to scale the loss for each pixel so that it can be applied to classification and regression tasks in a principled way. Further, the cosine similarity can be evaluated on the prediction scores for pixel-wise classification tasks and thereby leverage even more information from the network. Thus, CosPGD outperforms SegPGD by a significant margin when attacking semantic segmentation models.

3 Method

CosPGD is an iterative white-box attack that utilizes the pixel-wise cosine similarity to generate strong adversarial examples. The method is an effective extension of PGD for all pixel-wise predictions tasks with the same attack step as PGD, given by Equations (1), (2) & (3) and in [36, 22].

$$\mathbf{X}^{\text{adv}_{t+1}} = \mathbf{X}^{\text{adv}_t} + \alpha \cdot \text{sign} \nabla_{\mathbf{X}^{\text{adv}_t}} L(f_{\text{net}}(\mathbf{X}^{\text{adv}_t}), \mathbf{Y}) \quad (1)$$

$$\delta = \phi^\epsilon(\mathbf{X}^{\text{adv}_{t+1}} - \mathbf{X}^{\text{clean}}) \quad (2)$$

$$\mathbf{X}^{\text{adv}_{t+1}} = \phi^r(\mathbf{X}^{\text{clean}} + \delta) \quad (3)$$

where $\mathbf{X}^{\text{adv}_{t+1}}$ is a new adversarial example for time step $t+1$, generated using $\mathbf{X}^{\text{adv}_t}$, the adversarial example at time step t and initial clean sample $\mathbf{X}^{\text{clean}}$. \mathbf{Y} is the ground truth label for non-targeted attacks and the target for targeted attacks, α is the step size for the perturbation (multiplied by -1 for targeted attacks), and the function ϕ^ϵ is clipping the δ in ϵ -ball for l_∞ -norm bounded attacks or the ϵ -projection in l_2 -norm bounded attacks. Its purpose is to restrict the attack according to the l_∞ -norm or l_2 -norm constraints. ϕ^r is clipping the generated example in the valid input range (usually between $[0, 1]$). $\nabla_{\mathbf{X}^{\text{adv}_t}} L(\cdot)$ denotes the gradient of $\mathbf{X}^{\text{adv}_t}$ generated by backpropagating the loss and is used to determine the direction of the perturbation step. SegPGD [22] extends this formulation to tensor-valued predictions and labels $\mathbf{Y} \in \mathbb{R}^{H \times W \times M}$ for images of size $H \times W$ and categorical M output classes. This allows specifically optimizing perturbations on pixels on which the loss is low instead of only having access to the total loss per image.

Loss scaling in previous approaches When optimizing an adversarial attack, Gu et al. [22] argue that pixels which are already misclassified by the model are less relevant than pixels correctly classified by the model because the intention of the attack is to make the model misclassify as many pixels as possible while perturbing the δ inside the ϵ -ball. However, [22] argues that over iterations, as the number of misclassified pixels increases, the attack starts losing effectiveness if it only focuses on correctly classified pixels. Thus, Gu et al. [22] propose to scale the loss over iterations such that the scaling of the loss for correctly classified pixels is inversely proportional to the scaling of the loss for the incorrectly classified pixels. Initially, the loss for the correctly classified pixels is scaled higher, compared to the loss for the incorrectly classified pixels. Then, over iterations, the scaling of the loss for the correctly classified pixels is reduced (compare Equation (4) in SegPGD [23]). This avoids the concern of the attack becoming benign after a few iterations. However, splitting the pixels into two categories, *correctly* and *incorrectly* classified pixels, requires a fabricated global weighting of the scaling factor that decreases over the iterations to avoid numerical instabilities when many pixels are misclassified. Further, it limits the applicability of SegPGD to pixel-wise classification tasks like semantic segmentation by definition. For pixel-wise regression tasks like optical flow, and surface normal prediction such **an absolute measure of correctness would fail**. Further, comparing the pixel-wise labels after taking the argmax only provides limited information from the network prediction. Thus, we argue that the scope of the categories needs to be expanded such that it can encompass the similarity between the predictions and the label.

CosPGD The aim of the proposed CosPGD approach is to facilitate the effective application of PGD-like adversarial attacks to pixel-wise prediction tasks in a principled way. To cope with the above-sketched problem, we propose a unified way to scale the loss in classification and regression settings in a stable way. Specifically, for non-targeted settings, we aim to penalize pixel-wise in proportion to the pixel-wise predictions' similarity to the ground truth, while also accounting for the decrease in similarity over iterations. For targeted settings, we aim to penalize the dissimilarity of the prediction to the target prediction. We propose to use the cosine similarity as this measure, as it satisfies the desired properties.

The cosine similarity between the model predictions and target (ground truth) is calculated as shown in Equation (4) for each output pixel location:

$$\cos(\overrightarrow{\text{pred}}, \overrightarrow{\text{target}}) = \frac{\overrightarrow{\text{pred}} \cdot \overrightarrow{\text{target}}}{\|\overrightarrow{\text{pred}}\| \cdot \|\overrightarrow{\text{target}}\|} \quad (4)$$

Where, $\overrightarrow{\text{pred}}$ is the probability distribution of the predictions of a network $f_{\text{net}}(\cdot)$ for a position, and $\overrightarrow{\text{target}}$ is the distribution over the target predictions or ground truth at the same position. CosPGD

Algorithm 1 Algorithm for generating adversarial examples using CosPGD.

Require: model $f_{\text{net}}(\cdot)$, clean samples $\mathbf{X}^{\text{clean}}$, perturbation range ϵ , step size α , attack iterations T , ground truth \mathbf{Y}

$\mathbf{X}^{\text{adv}_0} = \mathbf{X}^{\text{clean}} + \mathcal{U}(-\epsilon, +\epsilon)$ \triangleright initialize adversarial example and clip to valid l_∞ or l_2 bound

for $t \leftarrow 1$ to T **do** \triangleright loop over attack iterations

$P = f_{\text{net}}(\mathbf{X}^{\text{adv}_{t-1}})$ \triangleright make predictions

$\text{cossim} \leftarrow \text{CosineSimilarity}(\Psi^*(P), \Psi'(\mathbf{Y}))$ \triangleright compute cosine similarity

if targeted attack:

$\text{cossim} \leftarrow 1 - \text{cossim}$ \triangleright punish dissimilarity to target

$\alpha \leftarrow -\alpha$ \triangleright opposite direction for targeted attack

$L_{\text{cos}} \leftarrow \text{cossim} \cdot L(P, \mathbf{Y})$ \triangleright scaling the pixel-wise loss for sample updates

$\mathbf{X}^{\text{adv}_t} \leftarrow \mathbf{X}^{\text{adv}_{t-1}} + \alpha \cdot \text{sign}(\nabla_{\mathbf{X}^{\text{adv}_{t-1}}} L_{\text{cos}})$ \triangleright update adversarial examples

$\delta \leftarrow \phi^\epsilon(\mathbf{X}^{\text{adv}_t} - \mathbf{X}^{\text{clean}})$ \triangleright clip δ to valid l_∞ or l_2 bound

$\mathbf{X}^{\text{adv}_{t+1}} = \phi^\epsilon(\mathbf{X}^{\text{clean}} + \delta)$ \triangleright add δ to $\mathbf{X}^{\text{clean}}$ and clip into valid image range

end for

as an untargeted attack, intends to drive the model's predictions away from the model's intended target(or ground truth). For pixel-wise prediction tasks like disparity estimation, optical flow, etc. the predictions, and targets are vectors containing information for each pixel. These are mapped to a distribution between $[0, 1]$.

In the case of semantic segmentation, we obtain the distribution target by generating a *one-hot encoded vector* of the target and we obtain the distribution over the predictions, by calculating the softmax of the predictions before taking the argmax as shown in Equation (5).

$$\overrightarrow{\text{pred}} = \text{softmax}(f_{\text{net}}(\mathbf{X})), \quad \text{softmax}(x_i) = \frac{\exp(x_i)}{\sum_j \exp(x_j)}. \quad (5)$$

Thus, in algorithm 1, Ψ^* is always the softmax function, and Ψ' is one-hot encoding in case of semantic segmentation while Ψ' is the softmax function when $\overrightarrow{\text{target}}$ is already a vector. Similar to [22], \mathbf{X}^{adv} is initialized to the clean input sample $\mathbf{X}^{\text{clean}}$ with added randomized noise in the range $[-\epsilon, +\epsilon]$, ϵ being the maximum allowed perturbation. Over attack iterations $\mathbf{X} = \mathbf{X}^{\text{adv}_t}$, the adversarial example generated at iteration t , such that $t \in [1, T]$, where T is the total number of attack iterations.

As discussed, we finally propose to scale the pixel-wise loss using this cosine similarity (cossim) $\cos(\overrightarrow{\text{pred}}, \overrightarrow{\text{target}})$, such that for the non-targeted setting, pixels where the network predictions are closer to the intended target (ground truth), have a higher similarity (approaching 1) and thus higher loss. Pixels with lower similarity, have a lower loss but are not rendered benign. While for the targeted setting, we consider the inverse of cosine similarities (refer Equation (7)), and thus, pixels where the network predictions are closer to the target, have higher similarity and thus lower loss, and pixels with lower similarity have a higher loss. Thus, the final loss over all pixels is calculated as shown in Equations (6) & (7). Then this loss is back propagated to obtain gradients over the sample to perform the adversarial attack as shown in Equation (3) using L_{cos} instead of L .

For non-targeted attacks:

$$L_{\text{cos}} = \frac{1}{H \times W} \sum_{H \times W} \cos(\overrightarrow{\text{pred}}, \overrightarrow{\text{target}}) \cdot L(f_{\text{net}}(\mathbf{X}^{\text{adv}_t}), \mathbf{Y}), \quad (6)$$

For targeted attacks:

$$L_{\text{cos}} = \frac{1}{H \times W} \sum_{H \times W} (1 - \cos(\overrightarrow{\text{pred}}, \overrightarrow{\text{target}})) \cdot L(f_{\text{net}}(\mathbf{X}^{\text{adv}_t}), \mathbf{Y}), \quad (7)$$

where H and W are the height and width of a sample \mathbf{X} . CosPGD is summarized in Algorithm 1.

4 Experiments

For demonstrating the wide applicability of CosPGD, we conduct our experiments on distinct downstream tasks: semantic segmentation, optical flow estimation, image restoration, and others. For semantic segmentation, we compare CosPGD to SegPGD and PGD, while for optical flow estimation and other tasks, we compare CosPGD to PGD. We can observe that CosPGD outperforms SegPGD and PGD, respectively.

4.1 Experimental setup

When comparing in the l_∞ -norm constraint, we use the same ϵ for CosPGD, SegPGD, and PGD i.e. $\epsilon \approx \frac{8}{255}$. For α , we follow the work by [22] and set the step size $\alpha = 0.01$. Further, when comparing in the l_2 -norm constraint, we follow common work [13, 55] and use the same ϵ for CosPGD, SegPGD, and PGD i.e. $\epsilon \approx \{\frac{64}{255}, \frac{128}{255}\}$ and $\alpha = \{\frac{25.5}{255}, \frac{51}{255}\}$. We show in supplementary material that CosPGD outperforms both PGD and SegPGD in the l_2 -norm constraint settings under all commonly used ϵ and α values.

Semantic Segmentation. We use the PASCAL VOC 2012 [16] dataset which contains 20 classes object classes and one background class, with 1464 training images, and 1449 validation images. We follow common practice [25, 22, 63, 64], and use work by Hariharan et al. [24], augmenting the training set to 10,582 images. We test on the validation dataset. Architectures used for our evaluations are UNet [46] with a ConvNeXt tiny encoder [38] (in supplementary material), and PSPNet [64] and DeepLabV3 [8] both with ResNet50 [26] encoders. We report the mean Intersection over Union (mIoU) and mean pixel accuracy (mAcc) as metrics for comparison.

Optical flow estimation. We use RAFT[52] for our evaluations and follow the evaluation procedure used by Teed and Deng [52]. Evaluations are performed on KITTI2015 [41] and MPI Sintel [6, 59] validation datasets. We use the networks pre-trained on FlyingChairs [15], and FlyingThings [40] and fine-tuned on training datasets of the specific evaluation, as provided by Teed and Deng [52]. For Sintel, we report the end-point error (*epe*) on both clean and final subsets, while for KITTI15 we report the *epe* and *epe-f1-all*.

Image Restoration. Chen et al. [9] in their work simplify a transformer-based architecture RestFormer[61] for image restoration tasks and first propose a simplified architecture as a Baseline network, and then improve upon it with intuitions backed by reasoning and ablation studies to propose Non-linear Activation Free Networks abbreviated as NAFNet. In this work, we perform adversarial attacks on both the Baseline network and NAFNet. Similar to [9], for the image-de-blurring task, we use the GoPro dataset[44] which consists of 3124 realistically blurry images of resolution 1280×720 and corresponding ground truth sharp images obtained using a high-speed camera. The images are split into 2103 training images and 1111 test images. For the image denoising task we use the Smartphone Image Denoising Dataset (SSID)[1]. This dataset consists of 160 noisy images taken from 5 different smartphones and their corresponding high-quality ground truth images. For both the image restoration tasks, we report the *PSNR* and *SSIM* scores of the reconstructed images w.r.t. to the ground truth images, averaged over all images. *PSNR* stands for Peak Signal-to-Noise ratio, a higher *PSNR* indicates a better quality image or an image closer to the image to which it is being compared. *SSIM* stands for Structural similarity[56].

Following common work [22, 48, 33], we focus on l_∞ -norm and l_2 -norm constrained **non-targeted** attacks for semantic segmentation. In principle, the benchmarking tool (algorithm) should extend to targeted settings. Thus, for optical flow estimation and image restoration, we focus on l_∞ -norm constrained targeted setting. We mean over multiple seeds to better comprehend the strengths of the attacks, especially due to the random noise added for all attacks during initialization.

4.2 Semantic Segmentation

We report the comparison of CosPGD to the recently proposed SegPGD and to PGD in Fig 2. We observe that using the cosine similarity between the distributions over the predictions and the targets yields a much stronger attack compared to naive equality between the predicted and target segmentation masks.

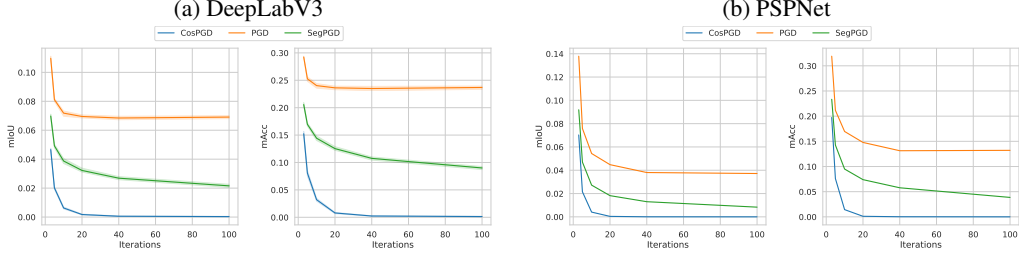


Figure 2: Comparison of performance of CosPGD to PGD and SegPGD for semantic segmentation over PASCAL VOC2012 validation dataset as l_∞ -norm constrained attacks using DeepLabV3 in fig.2a and PSPNet in fig.2b. We also report results in Table 1 in Section B.3.1.

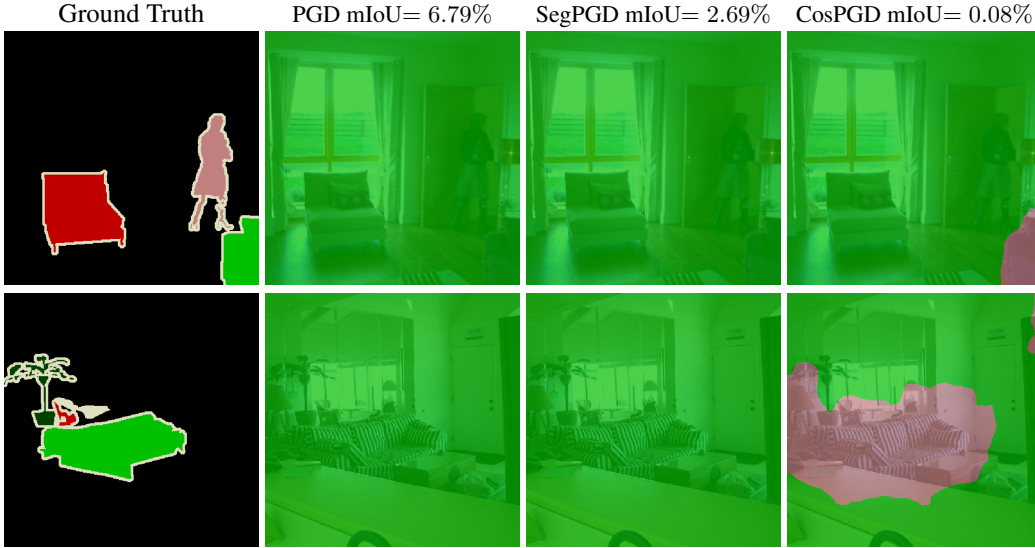


Figure 3: Comparing predictions of DeepLabV3 on PASCAL VOC 2012 validation dataset after PGD, SegPGD, and CosPGD attacks with 40 iterations. The ground truth segmentation masks are given on the left. We observe that both PGD and SegPGD are able to successfully change most of the image prediction, but not in the small region where the changed prediction mask is the same as the ground truth segmentation mask. Here, the superiority of CosPGD is aptly highlighted as it is able to change the prediction in this small region to a third class that does not exist in the image.

This is consistent across the number of attack iterations, as CosPGD fools the networks into making wrong predictions much better than SegPGD. This claim is supported by both metrics mIoU and mAcc being much lower for CosPGD when compared to SegPGD. Moreover, we note in Figure 3, that after 40 attack iterations, all attacks are considerably fooling the network into making incorrect predictions. However, once the dominant class label is changed by SegPGD or PGD, they do not further optimize over small regions of correct prediction. In contrast, CosPGD successfully fools the model into making incorrect predictions even in these small regions by either swapping the region prediction with an already existing class or forcing the model into predicting a class not existing in that sample. The merits of CosPGD and the demerits of SegPGD and PGD are qualitatively highlighted by Figure 3. While greedy approaches like PGD, originally designed for image classification tasks, are able to bring down the $mIoU$ of DeepLabV3 to 6.79%. A recent method, SegPGD by naively utilizing the pixel-wise loss, deteriorates the model performance further to 2.69%. However, CosPGD being more sophisticated is able to fool the network into making incorrect predictions for almost all pixels of the samples, by bringing down the model performance to 0.08% after 40 iterations and to approximately 0% after 100 attack iterations.

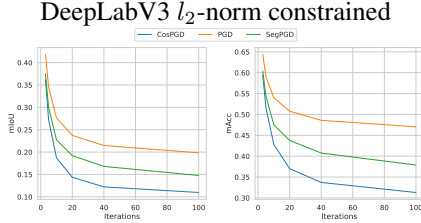


Figure 4: Comparison of L_2 -norm constrained CosPGD to PGD and SegPGD for semantic segmentation over PAS-CAL VOC2012 validation dataset using DeepLabV3. We provide attack results for all considered α and ϵ values in Section B.2.

extra L_∞ -norm and L_2 -norm constrained non-targeted adversarial attack results from Semantic Segmentation using the UNet architecture with ConvNeXt backbone on the **CityScapes** dataset[10] in Section B.1.

4.3 Optical Flow

For optical flow, we explore the l_∞ -norm constrained targeted setting. A comparison of CosPGD to PGD is shown in Figure 5. Here we quantitatively observe the better performance of CosPGD compared to PGD. As this is the targeted setting, we intend to close the gap between the target prediction and the model predictions, thus a lower *epe* of the model prediction w.r.t the target prediction is desired. As the attack iterations increase, across datasets, CosPGD is able to significantly fool the network into making predictions closer to the target, bringing down the *epe* to as low as 1.55 for Sintel (final). We observe qualitatively in Figure 6, the initial optical flow estimation by the model

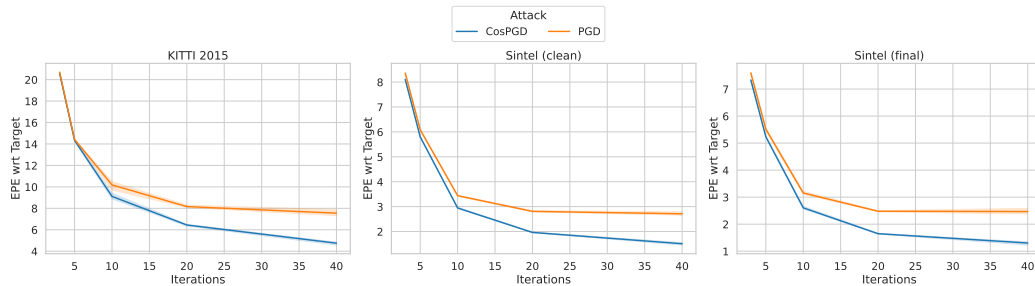


Figure 5: Comparison of performance of CosPGD to PGD for optical flow estimation over KITTI-2015 (left) and Sintel (clean \rightarrow centre and final \rightarrow right) validation datasets as l_∞ -norm constrained targeted attacks using RAFT. We observe, CosPGD as an attack is stronger than PGD. We also report these results in Table 2 in Section B.3.2.

(which is very different from the target) is only moderately changed when the model is attacked with a strong adversarial attack like PGD. As the attack was originally designed for classification tasks, the model is not significantly fooled even as the intensity of the attack is increased to 40 iterations.

Figure 6b, shows qualitatively that the model predictions are not significantly different from the initial predictions. The shape of the moving car is preserved to a considerable extent. The limited effectiveness of the PGD attack is further highlighted on increasing the attack strength to 40 iterations, in Figure 6c, some initial predictions are still preserved, for example, the bark of the tree. This is in contrast to when the model is attacked using CosPGD, a method that utilizes pixel-wise information. In Figure 6e, we observe that even at a low intensity of the attack (5 iterations), the model predictions are significantly different from the initial predictions, especially in the background and the shape of the moving car. The model is incorrectly predicting the motion of the pixels around the moving car. And at high attack intensity, as shown in Figure 6f with 40 iterations, the model’s optical flow

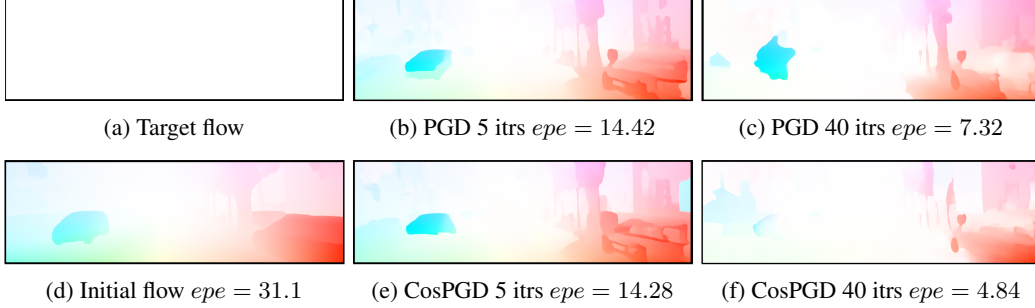


Figure 6: Comparing PGD and CosPGD as a targeted l_∞ -norm constrained attack on RAFT using KITTI15 validation set over various iterations. Fig.6a shows the targeted prediction, a $\vec{0}$ and fig.6d shows the initial optical flow estimation by the network before adversarial attacks. EPEs between the target and the final prediction are reported, thus lower epe is better. Figures 6b and 6c show flow predictions after PGD attack over 5 and 40 iterations respectively, while figures 6e and 6f show flow predictions after CosPGD attack over 5 and 40 iterations respectively. CosPGD significantly changes the overall structure of the optical flow field. Bringing is visibly closer to the targeted $\vec{0}$.

predictions are significantly inaccurate and exceedingly different from the initial predictions and very close to the target of $\vec{0}$. The model fails to differentiate the moving car from its background, moreover, the bark of the tree has completely vanished. In a real-world scenario, this vulnerability of the model to a relatively small perturbation ($\epsilon = \frac{8}{255}$) could be hazardous. A similar observation is made for the Sintel dataset, in Figure 1 (see Section 1). The dominance of CosPGD over PGD can be quantitatively observed in Figure 5 and the table provided in the supplementary material, demonstrating the effectiveness of the CosPGD attack for optical flow.

We provide extra results comparing CosPGD to PGD as a L_∞ -norm constrained non-targeted adversarial attack for optical flow estimation in Section C.1. Additionally, we also provide a comparison to PCFA [49] in Section C.3.

4.4 Image Restoration

Chen et al. [9] in their work show that NAFNet outperforms the Baseline network for image restoration tasks like image de-blurring and image denoising while both the Baseline network and NAFNet outperform the previous state-of-the-art methods.

However, the work does not compare the adversarial robustness of the networks, and as discussed in Section 1, adversarial robustness and generalization of networks are paramount for safety-critical applications. Thus, we compare the adversarial robustness of the two proposed networks and discuss the interesting findings.

In Figure 7 we observe for the Baseline network both CosPGD and PGD are performing at par while for the newly proposed NAFNet, PGD is still estimating its adversarial robustness to be very similar to the Baseline network and only after 20 attack iterations it is estimating correctly that NAFNet is not as robust as the Baseline network. However, CosPGD reveals that NAFNet is not as robust as the baseline even at less number of iterations. For the Baseline network we also observe that SegPGD is here is significantly weaker due to its limitation to image classification tasks as discussed in Section 3. However, for NAFNet, from 5 attack iterations onwards SegPGD is outperforming PGD, while still being weaker than CosPGD. This, interesting improvement in the performance of SegPGD as an adversarial attack can be attributed to the pixel-wise nature of the attack, similar to CosPGD further highlighting the benefits of utilizing pixel-wise information when crafting adversarial attacks for pixel-wise prediction tasks.

We report the experiments on image denoising task on SSID in Section C.2.

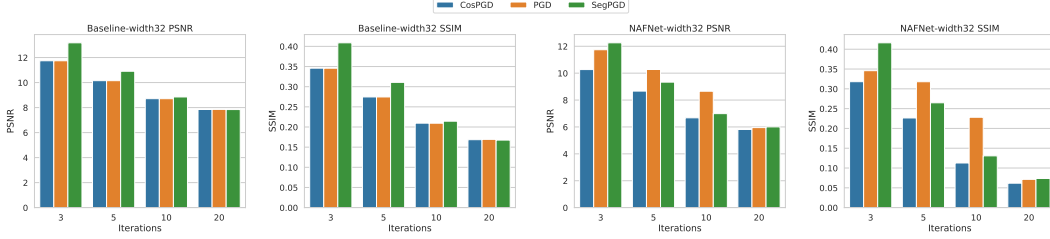


Figure 7: A Comparison of L_∞ -norm constrained non-targeted CosPGD, PGD, and SegPGD attacks on the Baseline network and NAFNet, both recently proposed by [9] as state-of-the-art networks for image restoration tasks like image de-blurring on GoPro dataset[44].

5 Conclusion

In this work, we demonstrated across different downstream tasks and architectures that our proposed adversarial attack, CosPGD, is significantly more effective than other existing and commonly used adversarial attacks on several pixel-wise prediction tasks. We provide a new benchmarking tool (algorithm) for the adversarial robustness of models on pixel-wise tasks. By comparing CosPGD to attacks like PGD that were originally proposed for image classification tasks, we expanded on the work by Gu et al. [22] and highlighted the need and effectiveness of attacks specifically designed for pixel-wise prediction tasks beyond segmentation. We illustrated the intuition behind using cosine similarity as a measure for generating stronger adversaries and leveraging more information from the model and backed it with experimental results from different downstream tasks. This further highlights the simplicity and principled formulation of CosPGD, thus making it applicable to a wide range of pixel-wise prediction tasks and in-principle extendable to all Lipschitz continuous bounds as a targeted or a non-targeted attack.

Limitations. Similar to most white-box adversarial attacks [21, 36, 39, 58, 22], CosPGD currently requires access to the model’s gradients for generating adversarial examples. While this is beneficial for generating adversaries, it limits the applications of the non-targeted settings as many benchmark datasets [41, 6, 59, 16] do not provide the ground truth for test data. Evaluations of the validation datasets certainly show the merit of the attack method. Yet, it would be interesting to study the attack on test images as well, due to the potential slight distribution shifts pre-existing in the test data. Additionally, there would exist settings, especially for non-targeted attacks where approaches like pixel-wise PGD would work at par with CosPGD as the *epe* can be increased equally by changing all pixel-wise regression estimates slightly or changing only a few of them drastically. We discuss this further in detail in Section C.

References

- [1] Abdelrahman Abdelhamed, Stephen Lin, and Michael S. Brown. A high-quality denoising dataset for smartphone cameras. In *2018 IEEE/CVF Conference on Computer Vision and Pattern Recognition*, pages 1692–1700, 2018. doi: 10.1109/CVPR.2018.00182.
- [2] Maksym Andriushchenko, Francesco Croce, Nicolas Flammarion, and Matthias Hein. Square attack: a query-efficient black-box adversarial attack via random search. 2020.
- [3] Anurag Arnab, Ondrej Miksik, and Philip H. S. Torr. On the robustness of semantic segmentation models to adversarial attacks, 2017. URL <https://arxiv.org/abs/1711.09856>.
- [4] Tom B. Brown, Dandelion Mané, Aurko Roy, Martín Abadi, and Justin Gilmer. Adversarial patch, 2017. URL <https://arxiv.org/abs/1712.09665>.
- [5] Vanessa Buhrmester, David Münch, and Michael Arens. Analysis of explainers of black box deep neural networks for computer vision: A survey, 2019. URL <https://arxiv.org/abs/1911.12116>.
- [6] D. J. Butler, J. Wulff, G. B. Stanley, and M. J. Black. A naturalistic open source movie for optical flow evaluation. In A. Fitzgibbon et al. (Eds.), editor, *European Conf. on Computer Vision (ECCV)*, Part IV, LNCS 7577, pages 611–625. Springer-Verlag, October 2012.

- [7] Nicholas Carlini and David Wagner. Towards evaluating the robustness of neural networks. In *2017 IEEE Symposium on Security and Privacy (SP)*, pages 39–57. IEEE, 2017.
- [8] Liang-Chieh Chen, George Papandreou, Florian Schroff, and Hartwig Adam. Rethinking atrous convolution for semantic image segmentation, 2017.
- [9] Liangyu Chen, Xiaojie Chu, Xiangyu Zhang, and Jian Sun. Simple baselines for image restoration, 2022.
- [10] Marius Cordts, Mohamed Omran, Sebastian Ramos, Timo Rehfeld, Markus Enzweiler, Rodrigo Benenson, Uwe Franke, Stefan Roth, and Bernt Schiele. The cityscapes dataset for semantic urban scene understanding, 2016.
- [11] Francesco Croce and Matthias Hein. Reliable evaluation of adversarial robustness with an ensemble of diverse parameter-free attacks. In *ICML*, 2020.
- [12] Francesco Croce and Matthias Hein. Mind the box: l_1 -apgd for sparse adversarial attacks on image classifiers. In *ICML*, 2021.
- [13] Francesco Croce, Maksym Andriushchenko, Vikash Sehwal, Nicolas Flammarion, Mung Chiang, Prateek Mittal, and Matthias Hein. Robustbench: a standardized adversarial robustness benchmark. *CoRR*, abs/2010.09670, 2020. URL <https://arxiv.org/abs/2010.09670>.
- [14] Francesco Croce, Maksym Andriushchenko, Vikash Sehwal, Edoardo Debenedetti, Nicolas Flammarion, Mung Chiang, Prateek Mittal, and Matthias Hein. Robustbench: a standardized adversarial robustness benchmark. In *Thirty-fifth Conference on Neural Information Processing Systems Datasets and Benchmarks Track (Round 2)*, 2021. URL <https://openreview.net/forum?id=SSKZPJt7B>.
- [15] A. Dosovitskiy, P. Fischer, E. Ilg, P. Häusser, C. Hazırbaş, V. Golkov, P. v.d. Smagt, D. Cremers, and T. Brox. FlowNet: Learning optical flow with convolutional networks. In *IEEE International Conference on Computer Vision (ICCV)*, 2015. URL <http://lmb.informatik.uni-freiburg.de/Publications/2015/DF15>.
- [16] M. Everingham, L. Van Gool, C. K. I. Williams, J. Winn, and A. Zisserman. The PASCAL Visual Object Classes Challenge 2012 (VOC2012) Results. <http://www.pascal-network.org/challenges/VOC/voc2012/workshop/index.html>.
- [17] Philipp Fischer, Alexey Dosovitskiy, Eddy Ilg, Philip Häusser, Caner Hazırbaş, Vladimir Golkov, Patrick van der Smagt, Daniel Cremers, and Thomas Brox. FlowNet: Learning optical flow with convolutional networks, 2015. URL <https://arxiv.org/abs/1504.06852>.
- [18] Shivangi Gajjar, Avik Hati, Shruti Bhilare, and Srimanta Mandal. Generating targeted adversarial attacks and assessing their effectiveness in fooling deep neural networks. In *2022 IEEE International Conference on Signal Processing and Communications (SPCOM)*, pages 1–5, 2022. doi: 10.1109/SPCOM55316.2022.9840784.
- [19] Robert Geirhos, Patricia Rubisch, Claudio Michaelis, Matthias Bethge, Felix A. Wichmann, and Wieland Brendel. Imagenet-trained cnns are biased towards texture; increasing shape bias improves accuracy and robustness, 2018. URL <https://arxiv.org/abs/1811.12231>.
- [20] Robert Geirhos, Jörn-Henrik Jacobsen, Claudio Michaelis, Richard Zemel, Wieland Brendel, Matthias Bethge, and Felix A. Wichmann. Shortcut learning in deep neural networks. *Nature Machine Intelligence*, 2(11):665–673, nov 2020. doi: 10.1038/s42256-020-00257-z. URL <https://doi.org/10.1038/s42256-020-00257-z>.
- [21] Ian J. Goodfellow, Jonathon Shlens, and Christian Szegedy. Explaining and harnessing adversarial examples, 2014. URL <https://arxiv.org/abs/1412.6572>.
- [22] Jindong Gu, Hengshuang Zhao, Volker Tresp, and Philip Torr. Segpgd: An effective and efficient adversarial attack for evaluating and boosting segmentation robustness. 2022. doi: 10.48550/ARXIV.2207.12391. URL <https://arxiv.org/abs/2207.12391>.
- [23] Jindong Gu, Hengshuang Zhao, Volker Tresp, and Philip Torr. Segpgd: An effective and efficient adversarial attack for evaluating and boosting segmentation robustness. page 5, 2022. doi: 10.48550/ARXIV.2207.12391. URL <https://arxiv.org/abs/2207.12391>.
- [24] Bharath Hariharan, Pablo Arbelaez, Lubomir Bourdev, Subhransu Maji, and Jitendra Malik. Semantic contours from inverse detectors. In *International Conference on Computer Vision (ICCV)*, 2011.

- [25] Bharath Hariharan, Pablo Arbeláez, Ross Girshick, and Jitendra Malik. Hypercolumns for object segmentation and fine-grained localization. In *2015 IEEE Conference on Computer Vision and Pattern Recognition (CVPR)*, pages 447–456, 2015. doi: 10.1109/CVPR.2015.7298642.
- [26] Kaiming He, Xiangyu Zhang, Shaoqing Ren, and Jian Sun. Deep residual learning for image recognition, 2015. URL <https://arxiv.org/abs/1512.03385>.
- [27] Dan Hendrycks and Thomas Dietterich. Benchmarking neural network robustness to common corruptions and perturbations, 2019. URL <https://arxiv.org/abs/1903.12261>.
- [28] Dan Hendrycks, Kevin Zhao, Steven Basart, Jacob Steinhardt, and Dawn Song. Natural adversarial examples, 2019. URL <https://arxiv.org/abs/1907.07174>.
- [29] Eddy Ilg, Nikolaus Mayer, Tonmoy Saikia, Margret Keuper, Alexey Dosovitskiy, and Thomas Brox. FlowNet 2.0: Evolution of optical flow estimation with deep networks, 2016. URL <https://arxiv.org/abs/1612.01925>.
- [30] Andrew Ilyas, Logan Engstrom, Anish Athalye, and Jessy Lin. Black-box adversarial attacks with limited queries and information. In *Proceedings of the 35th International Conference on Machine Learning, ICML 2018*, July 2018. URL <https://arxiv.org/abs/1804.08598>.
- [31] Mohit Iyyer, John Wieting, Kevin Gimpel, and Luke Zettlemoyer. Adversarial example generation with syntactically controlled paraphrase networks. In *Proceedings of the 2018 Conference of the North American Chapter of the Association for Computational Linguistics: Human Language Technologies, Volume 1 (Long Papers)*, pages 1875–1885, New Orleans, Louisiana, June 2018. Association for Computational Linguistics. doi: 10.18653/v1/N18-1170. URL <https://aclanthology.org/N18-1170>.
- [32] Daniel Kang, Yi Sun, Dan Hendrycks, Tom Brown, and Jacob Steinhardt. Testing robustness against unforeseen adversaries, 2019. URL <https://arxiv.org/abs/1908.08016>.
- [33] Xu Kang, Bin Song, Xiaojiang Du, and Mohsen Guizani. Adversarial attacks for image segmentation on multiple lightweight models. *IEEE Access*, 8:31359–31370, 2020. doi: 10.1109/ACCESS.2020.2973069.
- [34] Alex Krizhevsky, Ilya Sutskever, and Geoffrey E Hinton. Imagenet classification with deep convolutional neural networks. In F. Pereira, C.J. Burges, L. Bottou, and K.Q. Weinberger, editors, *Advances in Neural Information Processing Systems*, volume 25. Curran Associates, Inc., 2012. URL <https://proceedings.neurips.cc/paper/2012/file/c399862d3b9d6b76c8436e924a68c45b-Paper.pdf>.
- [35] Alexey Kurakin, Ian Goodfellow, and Samy Bengio. Adversarial examples in the physical world, 2016. URL <https://arxiv.org/abs/1607.02533>.
- [36] Alexey Kurakin, Ian Goodfellow, and Samy Bengio. Adversarial machine learning at scale, 2017.
- [37] Zhaoshuo Li, Xingtong Liu, Nathan Drenkow, Andy Ding, Francis X. Creighton, Russell H. Taylor, and Mathias Unberath. Revisiting stereo depth estimation from a sequence-to-sequence perspective with transformers. 2020. doi: 10.48550/ARXIV.2011.02910. URL <https://arxiv.org/abs/2011.02910>.
- [38] Zhuang Liu, Hanzi Mao, Chao-Yuan Wu, Christoph Feichtenhofer, Trevor Darrell, and Saining Xie. A convnet for the 2020s, 2022. URL <https://arxiv.org/abs/2201.03545>.
- [39] Aleksander Madry, Aleksandar Makelov, Ludwig Schmidt, Dimitris Tsipras, and Adrian Vladu. Towards deep learning models resistant to adversarial attacks, 2017. URL <https://arxiv.org/abs/1706.06083>.
- [40] N. Mayer, E. Ilg, P. Häusser, P. Fischer, D. Cremers, A. Dosovitskiy, and T. Brox. A large dataset to train convolutional networks for disparity, optical flow, and scene flow estimation. In *IEEE International Conference on Computer Vision and Pattern Recognition (CVPR)*, 2016. URL <http://lmb.informatik.uni-freiburg.de/Publications/2016/MIFDB16>. arXiv:1512.02134.
- [41] Moritz Menze and Andreas Geiger. Object scene flow for autonomous vehicles. In *Conference on Computer Vision and Pattern Recognition (CVPR)*, 2015.
- [42] Seyed-Mohsen Moosavi-Dezfooli, Alhussein Fawzi, and Pascal Frossard. Deepfool: a simple and accurate method to fool deep neural networks, 2015. URL <https://arxiv.org/abs/1511.04599>.
- [43] John X. Morris, Eli Lifland, Jin Yong Yoo, Jake Grigsby, Di Jin, and Yanjun Qi. Textattack: A framework for adversarial attacks, data augmentation, and adversarial training in nlp, 2020. URL <https://arxiv.org/abs/2005.05909>.

- [44] Seungjun Nah, Tae Hyun Kim, and Kyoung Mu Lee. Deep multi-scale convolutional neural network for dynamic scene deblurring. In *CVPR*, July 2017.
- [45] Marco Tulio Ribeiro, Sameer Singh, and Carlos Guestrin. Semantically equivalent adversarial rules for debugging NLP models. In *Proceedings of the 56th Annual Meeting of the Association for Computational Linguistics (Volume 1: Long Papers)*, pages 856–865, Melbourne, Australia, July 2018. Association for Computational Linguistics. doi: 10.18653/v1/P18-1079. URL <https://aclanthology.org/P18-1079>.
- [46] Olaf Ronneberger, Philipp Fischer, and Thomas Brox. U-net: Convolutional networks for biomedical image segmentation, 2015. URL <https://arxiv.org/abs/1505.04597>.
- [47] Jérôme Rony, Luiz G. Hafemann, Luiz S. Oliveira, Ismail Ben Ayed, Robert Sabourin, and Eric Granger. Decoupling direction and norm for efficient gradient-based l2 adversarial attacks and defenses, 2019.
- [48] Jérôme Rony, Jean-Christophe Pesquet, and Ismail Ben Ayed. Proximal splitting adversarial attacks for semantic segmentation, 2023.
- [49] Jenny Schmalfuss, Philipp Scholze, and Andrés Bruhn. A perturbation-constrained adversarial attack for evaluating the robustness of optical flow, 2022. URL <https://arxiv.org/abs/2203.13214>.
- [50] Simon Schrodli, Tonmoy Saikia, and Thomas Brox. Towards understanding adversarial robustness of optical flow networks. In *Proceedings of the IEEE/CVF Conference on Computer Vision and Pattern Recognition*, pages 8916–8924, 2022.
- [51] Yiming Sun, Feng Chen, Zhiyu Chen, and Mingjie Wang. Local aggressive adversarial attacks on 3d point cloud, 2021. URL <https://arxiv.org/abs/2105.09090>.
- [52] Zachary Teed and Jia Deng. Raft: Recurrent all-pairs field transforms for optical flow, 2020. URL <https://arxiv.org/abs/2003.12039>.
- [53] Berkay Mayalı username: mberkay0. mberkay0/pretrained-backbones-unet. <https://github.com/mberkay0/pretrained-backbones-unet>, 2023.
- [54] Johnson Vo, Jiabao Xie, and Sahil Patel. Multiclass asma vs targeted pgd attack in image segmentation, 2022. URL <https://arxiv.org/abs/2208.01844>.
- [55] Zekai Wang, Tianyu Pang, Chao Du, Min Lin, Weiwei Liu, and Shuicheng Yan. Better diffusion models further improve adversarial training, 2023.
- [56] Zhou Wang, A.C. Bovik, H.R. Sheikh, and E.P. Simoncelli. Image quality assessment: from error visibility to structural similarity. *IEEE Transactions on Image Processing*, 13(4):600–612, 2004. doi: 10.1109/TIP.2003.819861.
- [57] Alex Wong, Safa Cicek, and Stefano Soatto. Targeted adversarial perturbations for monocular depth prediction. In *Advances in neural information processing systems*, 2020.
- [58] Eric Wong, Leslie Rice, and J. Zico Kolter. Fast is better than free: Revisiting adversarial training, 2020. URL <https://arxiv.org/abs/2001.03994>.
- [59] J. Wulff, D. J. Butler, G. B. Stanley, and M. J. Black. Lessons and insights from creating a synthetic optical flow benchmark. In A. Fusiello et al. (Eds.), editor, *ECCV Workshop on Unsolved Problems in Optical Flow and Stereo Estimation*, Part II, LNCS 7584, pages 168–177. Springer-Verlag, October 2012.
- [60] Saining Xie, Ross Girshick, Piotr Dollár, Zhuowen Tu, and Kaiming He. Aggregated residual transformations for deep neural networks, 2016. URL <https://arxiv.org/abs/1611.05431>.
- [61] Syed Waqas Zamir, Aditya Arora, Salman Khan, Munawar Hayat, Fahad Shahbaz Khan, and Ming-Hsuan Yang. Restormer: Efficient transformer for high-resolution image restoration. In *CVPR*, 2022.
- [62] Jinlai Zhang, Lyujie Chen, Binbin Liu, Bo Ouyang, Qizhi Xie, Jihong Zhu, Weiming Li, and Yanmei Meng. 3d adversarial attacks beyond point cloud, 2021. URL <https://arxiv.org/abs/2104.12146>.
- [63] Hengshuang Zhao. semseg. <https://github.com/hszhao/semseg>, 2019.
- [64] Hengshuang Zhao, Jianping Shi, Xiaojuan Qi, Xiaogang Wang, and Jiaya Jia. Pyramid scene parsing network. In *CVPR*, 2017.

A Appendix

We include the following information in the supplementary material:

- Section A.1: We provide further experimental details.
- Section B.1: We provide extra L_∞ -norm and L_2 -norm constrained non-targeted adversarial attack results from Semantic Segmentation using the UNet architecture with ConvNeXt backbone on the **CityScapes** dataset[10].
- Section B.2: We provide extra L_2 -norm bounded non-targeted adversarial attack results from Semantic Segmentation using DeepLabV3 on the PASCAL VOC 2012 dataset.
- Section B.3: We report results from Figures 2 & 5 in a tabular form.
- Section C: We provide further discussion on limitations of CosPGD.
- Section C.1: We provide extra results comparing CosPGD to PGD as a L_∞ -norm constrained non-targeted adversarial attack for optical flow estimation.
- Section C.3: We provide a comparison to PCFA [49].

A.1 Further Experimental Details on Hardware and Metrics

Semantic Segmentation. For the experiments on DeepLabV3, we used NVIDIA Quadro RTX 8000 GPUs. For PSPNet, we used NVIDIA A100 GPUs. For the experiments with UNet, we used NVIDIA GeForce RTX 3090 GPUs. **Image Restoration.** For the experiments on Image de-blurring tasks, we used NVIDIA GeForce RTX 3090 GPUs.

A single GPU was used for each run.

Optical Flow Estimation. We used NVIDIA V100 GPUs, a single GPU was used for each run.

A.1.1 Calculating epe-f1-all.

Following the work by Teed and Deng [52], $f1 - all$ is calculated by averaging out over all the predicted optical flows. out is calculated using Equation (8),

$$out = epe > 3.0 \cup \frac{epe}{mag} > 0.05 \quad (8)$$

Where, $mag = \sqrt{flow \ ground \ truth^2}$

B Experimental Results

B.1 Semantic Segmentation with UNet on Cityscapes

In the following, we provide extra results on semantic segmentation with UNet on the Cityscapes dataset.

B.1.1 Experimental Setup.

In this evaluation, we use a UNet architecture [46] with a ConvNeXt_tiny encoder[38]. We extend the implementation from [53] to implement CosPGD, PGD, and SegPGD non-targeted L_∞ -norm and L_2 -norm attacks.

We do these evaluations on the Cityscapes dataset [10]. Cityscapes contains a total of 5000 high-quality images and pixel-wise annotations for urban scene understanding. The dataset is split into 2975, 500, and 1525 images for training, validation, and testing respectively. The model is trained on the test split and attacks are evaluated on the validation split.

B.1.2 Experimental Results and Discussion.

In Figure 8, we report results from the comparison of non-targeted CosPGD to PGD and SegPGD attacks across iterations and across L_p -norm constraints: L_∞ -norm and L_2 -norm using UNet architecture with a ConvNeXt tiny encoder on Cityscapes validation dataset. For the L_∞ -norm constraint,

we use the same $\alpha = 0.01$ and $\epsilon \approx \frac{8}{255}$ as in all previous evaluations. For the L_2 -norm constraint we follow common work [13, 55] and use the same ϵ for CosPGD, SegPGD, and PGD i.e. $\epsilon \approx \{\frac{64}{255}, \frac{128}{255}\}$ and $\alpha = \{0.1, 0.2\}$.

Note, SegPGD has been proposed as an L_∞ -norm constrained attack. We extend it to the L_2 -norm constraint merely for complete comparison and curiosity.

We observe in Figure 8 that CosPGD is a significantly stronger attack than both PGD and SegPGD, across iterations and L_p -norm constraints, and α and ϵ values. Especially as an L_2 -norm constrained attack, as shown before in Figure 4 for DeepLabV3 on PASCAL VOC 2012 dataset and discussed before in Section 4.2, as attack iterations, CosPGD is able to increase the gap in performance quite significantly.

B.2 Semantic Segmentation with DeepLabV3: Extra results

Further in Figure 9, we extend the results from Figure 4, to report L_2 -norm constrained attack evaluations on commonly used [13, 55] values of $\epsilon \approx \{\frac{64}{255}, \frac{128}{255}\}$ and $\alpha = \{0.1, 0.2\}$.

B.3 Tabular Results.

Here we report the quantitative results that have already been presented in the main paper in Figures 2 & 5 in tabular form.

B.3.1 Semantic Segmentation

For the results reported in Figure 2, we report the results in tables 1.

Table 1: Comparison of performance of CosPGD to SegPGD for semantic segmentation over PASCAL VOC2012 validation dataset. We observe that CosPGD is a significantly stronger attack compared to SegPGD for both metrics, and all models.

Network	Attack method	Attack iterations											
		3		5		10		20		40		100	
		mIoU(%)	mAcc(%)	mIoU(%)	mAcc(%)	mIoU(%)	mAcc(%)	mIoU(%)	mAcc(%)	mIoU(%)	mAcc(%)	mIoU(%)	mAcc(%)
UNet	SegPGD	12.38	32.41	7.75	25.27	4.46	18.36	2.98	14.24	2.20	11.66	1.55	8.66
	CosPGD	9.67	29.46	3.71	15.89	0.61	3.39	0.06	0.38	0.03	0.16	0.01	0.04
PSPNet	PGD	13.79	31.91	7.59	21.15	5.44	16.96	4.48	14.78	3.80	13.13	3.72	13.21
	SegPGD	9.19	23.25	4.7	14.25	2.72	9.5	1.82	7.39	1.3	5.77	0.83	3.86
	CosPGD	7.03	19.73	2.15	7.6	4.08	1.44	0.04	0.11	0.005	0.021	0.0002	0.0007
DeepLabV3	PGD	10.69	28.76	8.0	25.29	7.02	24.05	6.84	23.87	6.79	23.81	7.01	24.13
	SegPGD	6.76	19.78	4.86	16.49	3.84	14.29	3.31	12.40	2.69	10.81	2.15	9.25
	CosPGD	4.44	14.97	1.84	7.89	0.69	3.18	0.12	0.48	0.08	0.25	0.005	0.16

B.3.2 Optical flow estimation

Table 2: Comparison of performance of CosPGD to PGD as a targeted attack for optical flow estimation over KITTI15 and Sintel validation datasets using RAFT for different numbers of attack iterations. epe values are compared, with respect to both, the **Target** i.e. $\vec{0}$ where a lower epe indicates a better attack and Initial flow prediction (optical flow estimated by the model before any adversarial attack) where a higher epe indicates a better attack. CosPGD and PGD perform similarly for a low number of iterations, where CosPGD fits the target slightly better. CosPGD significantly outperforms PGD from the 10th iteration on on both metrics.

Attack	KITTI 2015				MPI Sintel							
	PGD		CosPGD		clean				final			
	Target↓	Initial↑	Target↓	Initial↑	Target↓	Initial↑	Target↓	Initial↑	Target↓	Initial↑	Target↓	Initial↑
3	20.7	11.4	20.6	11.2	8.3	6.8	8.1	6.6	7.6	7.3	7.5	7.3
5	14.4	17.8	14.3	17.7	6.1	9.0	5.8	8.8	5.6	9.4	5.2	9.3
10	10.5	22.1	9.0	23.4	3.4	11.2	2.9	11.4	3.1	11.3	2.6	11.5
20	8.1	24.6	6.5	25.8	2.8	11.7	2.0	12.1	2.5	11.8	1.6	12.1
40	7.3	25.0	4.8	27.4	2.8	11.7	1.6	12.4	2.6	12.3	1.3	12.3

Here we report the results from Figure 5 comparing CosPGD to PGD as a targeted attack using RAFT for KITTI15 and Sintel datasets in tabular form in Table 2. We observe that CosPGD is more effective than PGD to change the predictions toward the targeted prediction. During a low number of iterations

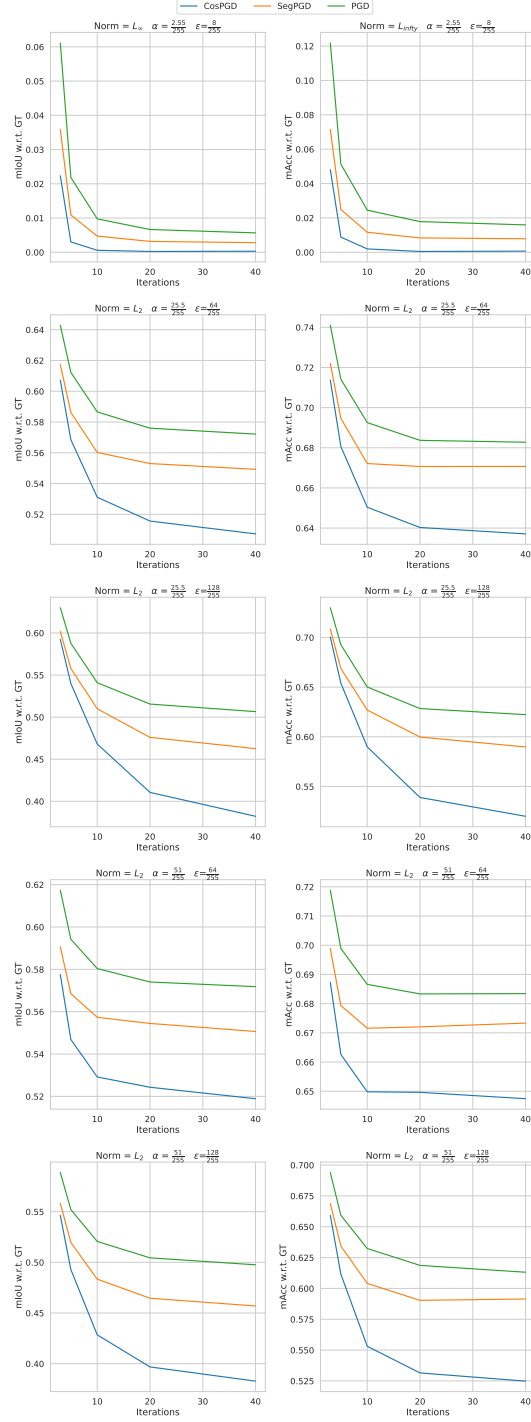


Figure 8: Comparing non-targeted CosPGD to PGD and SegPGD attacks across iterations and L_p -norm constraints, and α and ϵ values using UNet architecture with a ConvNeXt tiny encoder on Cityscapes validation dataset.

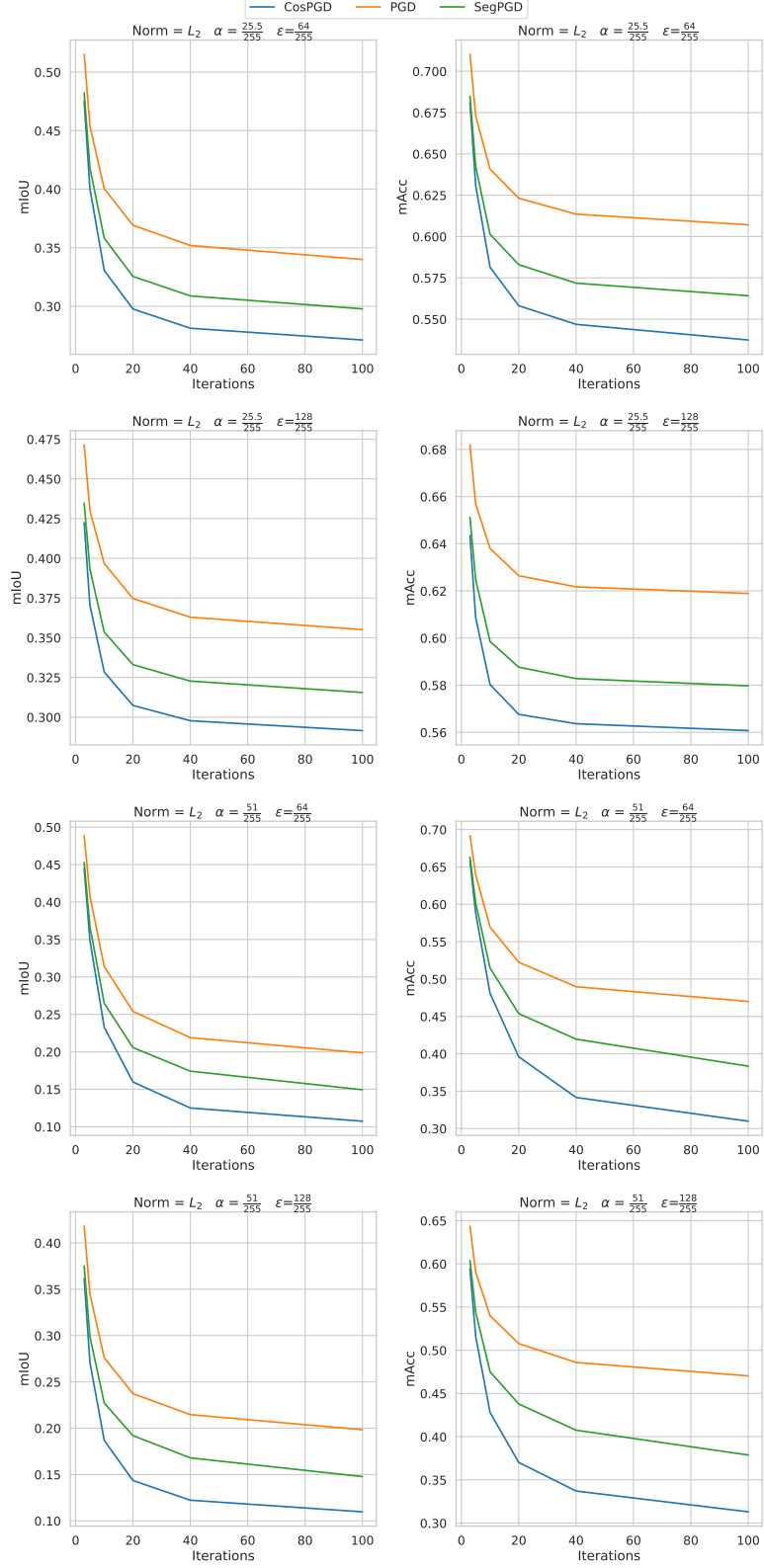


Figure 9: Comparing CosPGD to PGD and SegPGD across iterations as L_2 -norm constrained attacks, and across α and ϵ values using DeepLabV3 architecture with a ResNet50 on PASCAL VOC 2012 validation dataset.

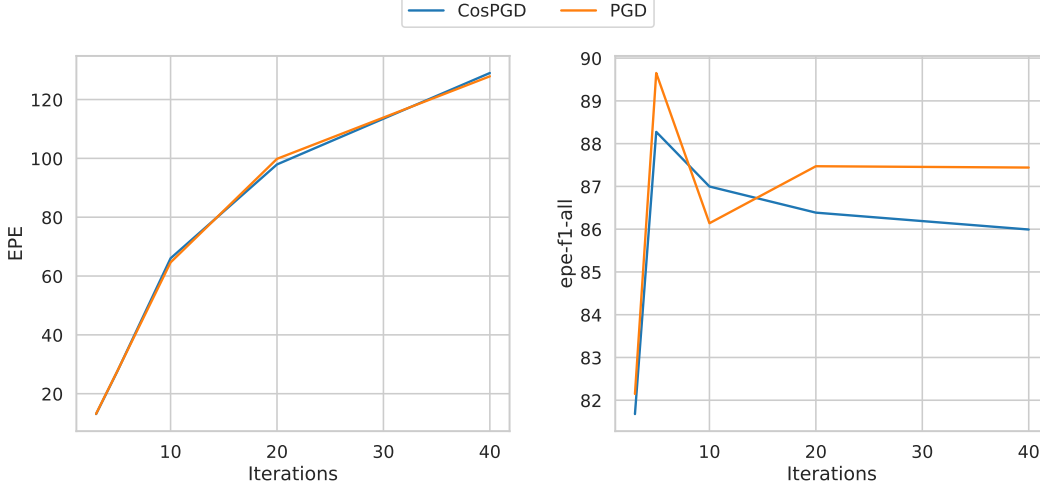


Figure 10: Comparing CosPGD and PGD as L_∞ -norm constrained non-targeted attacks for optical flow estimation using RAFT on KITTI 2015 validation dataset.

(iterations = 3 and 5), PGD is on par with CosPGD in increasing the *epe* values of the predictions compared to the initial predictions on non-attacked images. However, as the number of iterations increases, CosPGD outperforms PGD for this metric as well.

C Further discussion on limitations of CosPGD

As discussed in Section 5 paragraph Limitations, there would exist settings where approaches like pixel-wise PGD work at par with CosPGD as the *epe* can be changed equally by changing all pixel-wise regressing estimates slightly or changing only a few of them drastically. Here, we explore this limitation further and also compare CosPGD to a recently proposed sophisticated L_2 -norm constrained targeted attack PCFA.

C.1 Non-targeted attacks for optical flow estimation

For L_∞ -norm constrained non-targeted attacks, CosPGD changes pixels values temperately over a larger region of the image, while PGD changes it drastically but only for a small region in the image. This can be observed in Figure 10 when CosPGD and PGD are compared as L_∞ -norm constrained non-targeted attacks for optical flow estimation. We observe that both CosPGD and PGD are performing at par as both have very similar *epe* values across iterations. However, CosPGD across iterations has a lower *epe-f1-all* value. As shown by Equation 8 in Section A.1.1, *epe-f1-all* is the measure of average over all *epe* values that are above a modest threshold. Therefore, both CosPGD and PGD have very similar *epe* scores while CosPGD has a significantly lower *epe-f1-all* compared to PGD. This implies that CosPGD and PGD are performing at par, however PGD is drastically changing *epe* values at certain pixels, while CosPGD is changing *epe* values temperately over considerably more pixels. Figure 11 shows this qualitatively for 4 randomly chosen samples.

C.2 Non-targeted attacks for image denoising task

Further extending the findings from Section C.1 we report L_∞ -norm constrained non-targeted attacks for the image denoising using Baseline network and NAFNet in Figure. 12. We observe that both CosPGD and PGD are performing at par for both, the Baseline network and NAFNet. Additionally, similar to findings in Section 4.4, SegPGD is unable to perform at par with CosPGD and PGD.

C.3 Comparison to PCFA

Further, we compare CosPGD as a L_2 -norm constrained targeted attack to the recently proposed *state-of-the-art* L_2 -norm constrained targeted attack PCFA[49]. For comparison. we use the same

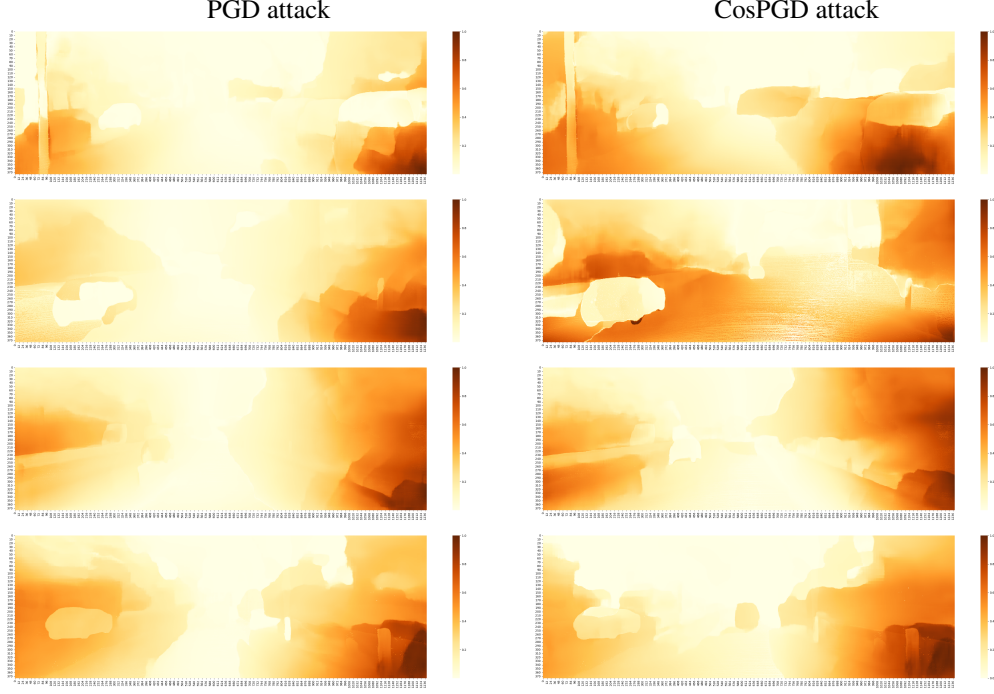


Figure 11: Comparing change in pixel-wise epe values w.r.t. initial epe values after 40 iterations of PGD and CosPGD as non-targeted l_∞ -norm constrained attacks on RAFT using KITTI15 validation set. The values for each image are: $\frac{|epe_{adv} - epe_{initial}|}{\max(epe_{adv})}$ where epe_{adv} & $epe_{initial}$ are pixel-wise epe values of the final adversarial sample and the initial non-attacked image, respectively.

settings as those used by the authors for both the attacks, for 20 attack iterations (steps), generating adversarial patches for each image individually, bounded under the change of variables methods proposed by Schmalfluss et al. [49]. Here, we observe that a sophisticated L_2 -norm constrained targeted attack, PCFA that does not utilise pixel-wise information for generating adversarial patches over all considered networks and datasets, performs similar to CosPGD. We consider both targeted settings proposed by Schmalfluss et al. [49], i.e. target being a zero vector($\vec{0}$) and target being the negative of the initial prediction(*negative flow*). We compare the average epe over all images. A lower AEE is w.r.t. Target and higher AEE w.r.t. initial indicate a stronger attack. Figure 13, provides an overview of the comparison between the two methods, using targets as $\vec{0}$ and *negative flow*. Figures 14, 15, provide further details compares both methods when using $\vec{0}$ and *negative flow* as the target, respectively.

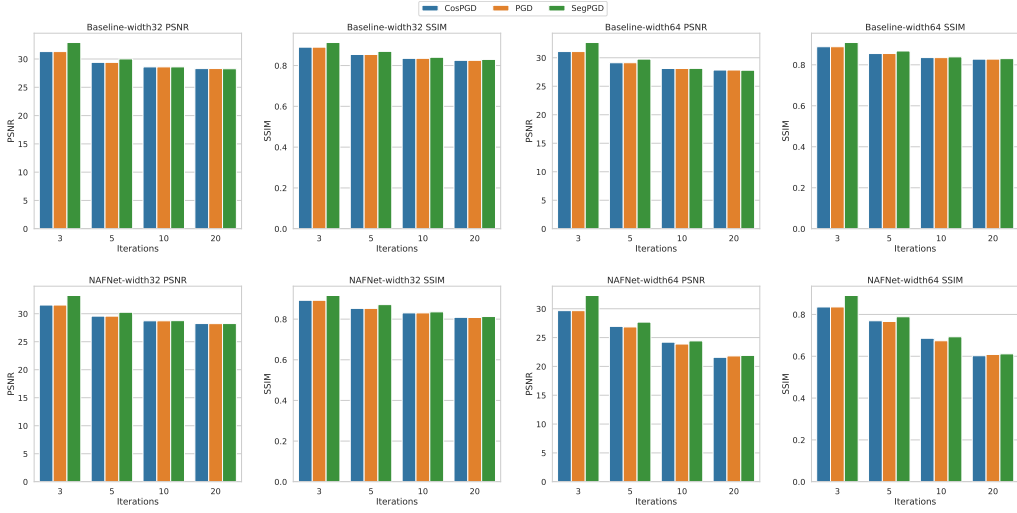


Figure 12: Comparing CosPGD to PGD and SegPGD as L_∞ -norm constrained non-targeted attacks for the image denoising task using Baseline network (top row) and NAFNet (bottom row) on SSID dataset. A lower value of PSNR and SSIM indicate a stronger attack.

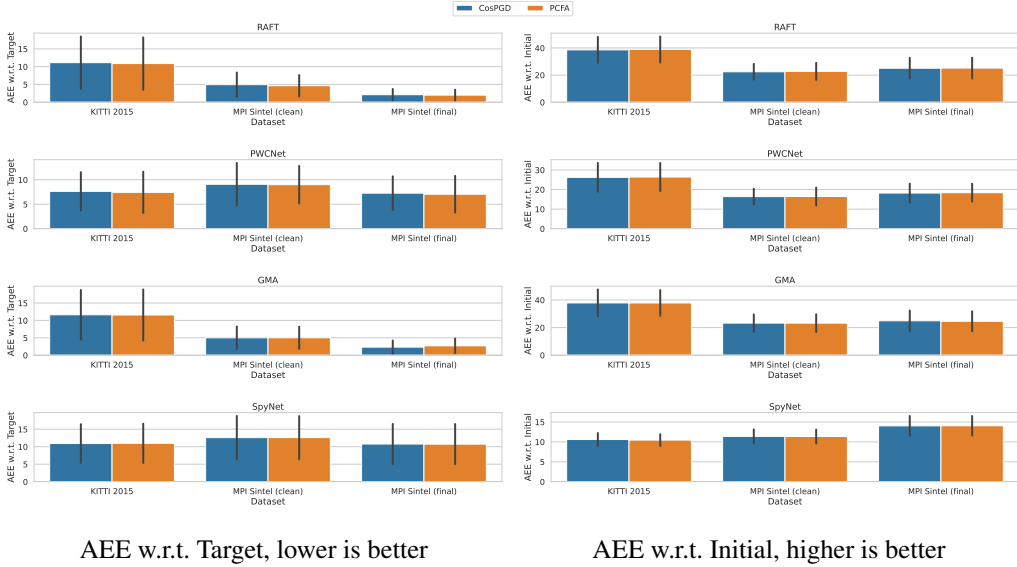
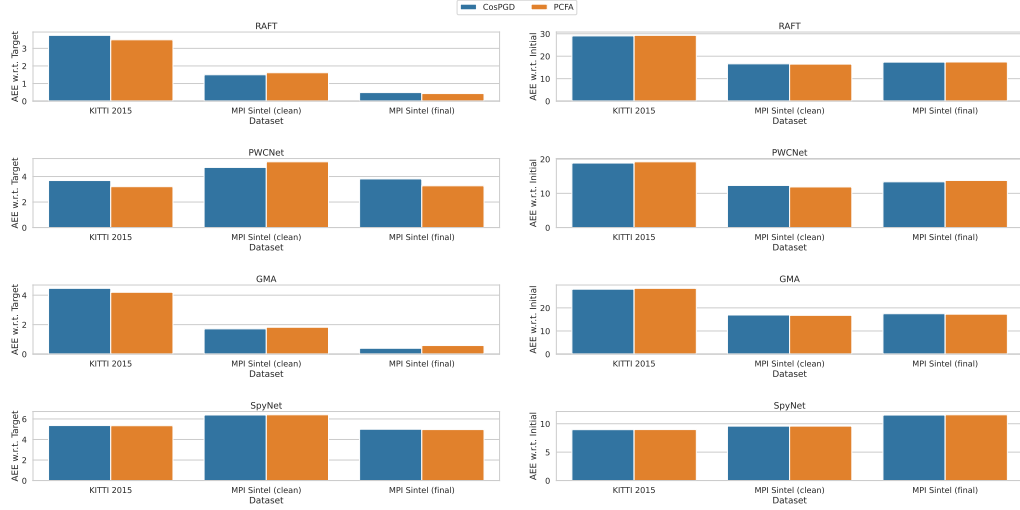


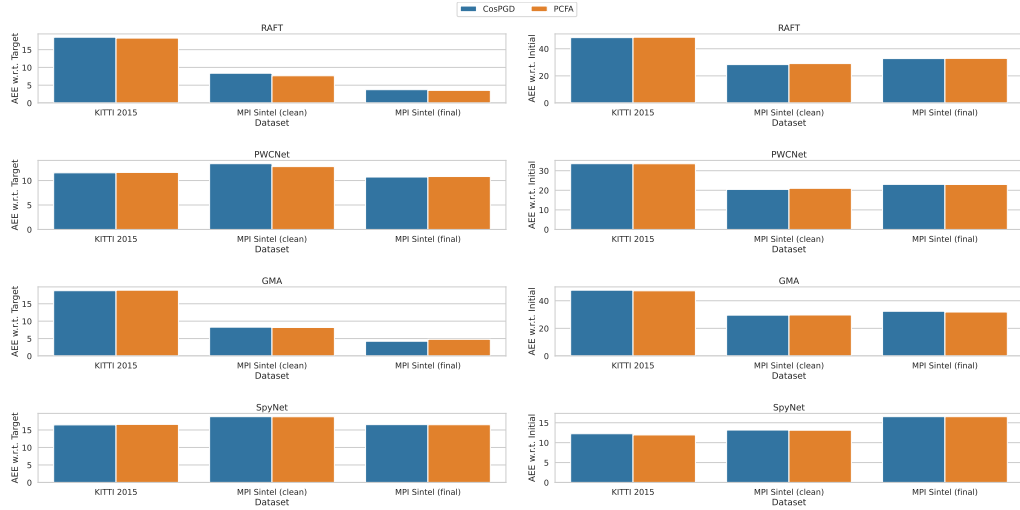
Figure 13: Comparison of mean and standard deviation of the results using different targets, $\vec{0}$ and *negative flow* for CosPGD and PCFA. A lower *AEE* is w.r.t. Target and a higher *AEE* w.r.t. initial indicate a stronger attack.



AEE w.r.t. Target, lower is better

AEE w.r.t. Initial, higher is better

Figure 14: Comparison of PCFA and CosPGD when using $\vec{0}$ as the target. A lower AEE is w.r.t. Target and a higher AEE w.r.t. initial indicate a stronger attack.



AEE w.r.t. Target, lower is better

AEE w.r.t. Initial, higher is better

Figure 15: Comparison of PCFA and CosPGD when using *negative flow* as the target. A lower AEE is w.r.t. Target and a higher AEE w.r.t. initial indicate a stronger attack.